Environmental Pollution 317 (2023) 120625

Contents lists available at ScienceDirect

Environmental Pollution

journal homepage: www.elsevier.com/locate/envpol

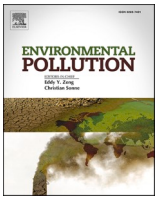

A novel toxic effect of foodborne trichothecenes: The exacerbation of genotoxicity☆

Marion Garofalo [a,b], Delphine Payros [a,b], Marie Penary [b], Eric Oswald [b,c], Jean-Philippe Nougayrède [b,1], Isabelle P. Oswald [a,*,1]

[a] Toxalim (Research Centre in Food Toxicology), Université de Toulouse, INRAE, ENVT, INP-Purpan, UPS, Toulouse, France
[b] IRSD, Université de Toulouse, INSERM, INRAE, ENVT, UPS, Toulouse, France
[c] CHU Toulouse, Hôpital Purpan, Service de Bactériologie-Hygiène, Toulouse, France

ARTICLE INFO

Keywords:
Mycotoxins
Pesticides
Microbiota
Colibactin
Carcinogenic potential

ABSTRACT

Trichothecenes (TCT) are very common mycotoxins. While the effects of DON, the most prevalent TCT, have been extensively studied, less is known about the effect of other trichothecenes. DON has ribotoxic, pro-inflammatory, and cytotoxic potential and induces multiple toxic effects in humans and animals. Although DON is not genotoxic by itself, it has recently been shown that this toxin exacerbates the genotoxicity induced by model or bacterial genotoxins. Here, we show that five TCT, namely T-2 toxin (T-2), diacetoxyscirpenol (DAS), nivalenol (NIV), fusarenon-X (FX), and the newly discovered NX toxin, also exacerbate the DNA damage inflicted by various genotoxins. The exacerbation was dose dependent and observed with phleomycin, a model genotoxin, captan, a pesticide with genotoxic potential, and colibactin, a bacterial genotoxin produced by the intestinal microbiota. For this newly described effect, the trichothecenes ranked in the following order: T-2>DAS > FX > NIV ≥ DON ≥ NX. The genotoxic exacerbating effect of TCT correlated with their ribotoxic potential, as measured by the inhibition of protein synthesis. In conclusion, our data demonstrate that TCT, which are not genotoxic by themselves, exacerbate DNA damage induced by various genotoxins. Therefore, foodborne TCT could enhance the carcinogenic potential of genotoxins present in the diet or produced by intestinal bacteria.

1. Introduction

Mycotoxins are the most prevalent natural dietary toxins and contaminate up to 70% of global crop production (Eskola et al., 2020). They represent a major issue for food safety (Payros et al., 2021a). These secondary metabolites, produced by microscopic fungi, resist industrial processes and cooking, and contaminate finished processed food. Trichothecenes (TCT) are one of the most prevalent types of mycotoxins, which include over 200 structurally related compounds with a common sesquiterpenoid skeleton (Polak-Śliwińska and Paszczyk, 2021). The differences in their substitution patterns allow TCT to be classified into four subgroups. Type A TCT (TCT-A) and type B TCT (TCT-B) are major food contaminants, whereas type C and D TCT rarely occur in food matrices. Type D TCT have attracted more attention as indoor pollutants (Gottschalk et al., 2008). TCT-A include T-2 toxin (T-2), diacetoxyscirpenol (DAS), and the newly discovered NX toxin (Varga et al., 2015; Pierron et al., 2022). TCT-B, distinguishable from TCT-A due to the presence of ketonic oxygen at C-8, are mainly represented by deoxynivalenol (DON), nivalenol (NIV), or fusarenon-X (FX) (Fig. 1). In Europe, almost 50% of cereals are contaminated with DON (Knutsen et al., 2017a), 16% with NIV (Knutsen et al., 2017b), and 10% with FX (Schothorst et al., 2003). T-2 was detected in 20% of European cereal samples (Knutsen et al., 2017c) and DAS was detected in 1.5% of European cereals and cereal-based food (Knutsen et al., 2018).

The toxicity of DON, the most prevalent foodborne TCT, is well documented. Acute DON poisoning causes vomiting, nausea, and diarrhoea, while chronic exposure results in food refusal, anorexia, reduced body weight gain, and altered immune responses (Terciolo et al., 2018; Pinton and Oswald, 2014; Payros et al. 2016). At the cellular level, DON triggers ribotoxicity, signalled by protein translation arrest and recruitment of MAP kinases, resulting in inflammation, cytotoxicity, and apoptosis, depending on the dose and duration of exposure (Payros

☆ This paper has been recommended for acceptance by Dr Mingliang Fang.

* Corresponding author.
E-mail address: isabelle.oswald@inrae.fr (I.P. Oswald).

[1] Co senior authors.

https://doi.org/10.1016/j.envpol.2022.120625
Received 18 August 2022; Received in revised form 25 October 2022; Accepted 7 November 2022
Available online 18 November 2022

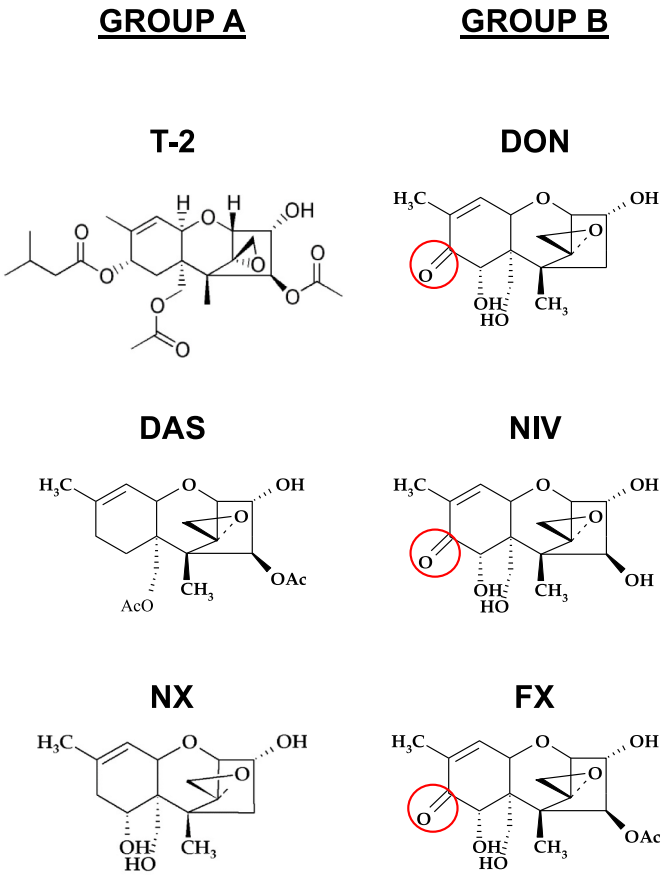

Fig. 1. Chemical structures of trichothecenes. Dietary TCT are classified in two main groups. Group A TCT include T-2 toxin (T-2), diacetoxyscirpenol (DAS), and NX. Groupe B TCT include deoxynivalenol (DON), nivalenol (NIV), and fusarenon-X (FX). Group A TCT can be distinguished from group B TCT by the presence of a C_8 keto-oxygen (circled in red). (For interpretation of the references to colour in this figure legend, the reader is referred to the Web version of this article.)

et al., 2016; Alassane-Kpembi et al., 2013; Payros et al., 2021b). By contrast, other TCT are largely overlooked in toxicology studies (Seeboth et al., 2012; Alassane-Kpembi et al., 2017a; Alassane-Kpembi et al., 2017b; Pierron et al., 2022). Additional studies are needed, both because these TCT are widely distributed in food, and because they induce not only effects similar to DON, such as ribotoxicity, cytotoxicity, inflammation, vomiting, and food refusal, but also specific effects. For example, T-2 induces an oral irritant effect with skin blistering (Wyatt et al., 1973), FX exhibits potent antiviral properties (Tani et al., 1995), DAS induces intestinal cell hyperplasia (Weaver et al., 1981), NIV triggers murine dendritic cell necrosis, which has not been documented for other TCT (Luongo et al., 2010), and NX specifically targets the mitochondria (Soler et al., 2022). The differences between TCT are also at the molecular level, with differences in the translation step that they inhibit. Although all TCT are thought to inhibit peptide elongation (Foroud et al., 2019), T-2, DAS, NIV, and FX also inhibit the initiation step, and DON and FX also inhibit translation termination (Cundliffe and Davies, 1977).

DON, which is not genotoxic on its own, has recently been described as capable of increasing the genotoxicity induced by model or bacterial genotoxins (Payros et al., 2017; Garofalo et al., 2022). This effect is observed with genotoxins with different modes of action, and a role for ribotoxicity has been proposed (Garofalo et al., 2022). In this work, we show that the genotoxicity exacerbation is not only an effect caused by DON, but also caused by T-2, DAS, NIV, FX, and NX. Importantly, TCT do not only exacerbate the genotoxicity induced by a model genotoxin, but they also exacerbate the genotoxicity induced by captan, a pesticide contaminating the food, and by colibactin, a genotoxin produced by *Escherichia coli* bacteria in the gut. Thus, although TCT are not genotoxic, they could enhance the carcinogenic potential of genotoxins present in the diet or in our microbiota.

2. Methods

2.1. Toxins and reagents

DON, NIV, T-2, FX, and DAS were purchased from Sigma-Aldrich (Saint-Quentin Fallavier, France) and captan was purchased from Dr. Ehrenstorfer (GmbH, Germany/CIL-Cluzeau). Phleomycin (PHM) (13.78 mM) was purchased from Invivogen (Toulouse, France). NX, obtained following the methods described by Aitken et al., was a generous gift from D. J. Miller (Aitken et al., 2019). Stock solutions were stored at −20 °C. DON (5 mM), NIV (30 mM), T-2 (5 mM), FX (10 mM), DAS (3 mM), and captan (50 mM) were dissolved in DMSO; NX (5 mM) was dissolved in water.

2.2. Cell culture and treatments

Non-transformed rat intestinal epithelial cells (IEC-6, ATCC CRL-1592) were incubated in complete DMEM medium supplemented with 10% foetal calf serum, 1% non-essential amino acids (Fisher scientific, Hampton, USA), and 0.1 U/mL bovine insulin (Sigma- Aldrich), at 37 °C with 5% CO_2. The cells were split regularly to maintain exponential growth. A fresh culture was created from a liquid nitrogen stock every 30 passages. The cells were confirmed free of mycoplasma contamination by 16 S PCR. For viability assay, cells were seeded in white 96 well plates (Dutscher, Bruxelles, Belgium) and grown to reach ~80% confluence. Cells were then treated for 4 h, 8 h or 24 h with various doses of TCT (or DMSO vehicle) before viability was measured. For ribotoxicity and γH2AX measurement by In-Cell-Western, cells were seeded in black 96 well plates (Greiner bio-one, Les Ulis, France) and grown to reach ~80% confluence. For ribotoxicity measurement, cells were incubated for 4 h with various doses of TCT or DMSO vehicle followed by a 30 min incubation with puromycin (Sigma-Aldrich) at a final concentration of 10 μg/mL. For immunofluorescence microscopy, cells were seeded in slide chambers (LabTek) and grown to reach ~80% confluence before treatment. For PHM and captan-induced genotoxicity measurement, cells were co-treated for 4 h with 5 μM PHM or 5–10 μM of captan and various doses of TCT.

2.3. Cell infection with colibactin-producing bacteria

Colibactin is highly unstable and thus detection of its genotoxicity requires its production *de novo* by the bacteria in close proximity with the epithelial cells (Chagneau et al., 2022). The intestinal carcinogenic *E. coli* strain NC101 that produces the genotoxin colibactin, and the isogenic mutant strain NC101Δ*clbP,* which does not produce the toxin (Yang et al., 2020) were cultured in Lysogeny-broth (LB) Lennox medium overnight at 37 °C with shaking. 500 μL of the LB culture was then inoculated in 9,5 mL of pre-warmed interaction medium DMEM with 25 mM Hepes (Fisher scientific) and grown at 37 °C with shaking until the culture reached an optical density (OD) at 600 nm of 0.5. IEC-6 cells were washed 3 times with warm HBSS (Fisher scientific), and HBSS was replaced by DMEM Hepes interaction medium, supplemented or not with various doses of TCT. Then, the bacteria were added with a multiplicity of infection (MOI, number of bacteria per cell) of 10. The cells were infected for 4 h at 37 °C with 5% CO_2. Then, the cells were carefully washed 3 to 5 times with warm HBSS and incubated in complete DMEM medium (supplemented with 200 μg/mL gentamycin to kill remaining bacteria), ± TCT for 4 h, and then processed for In-Cell-Western or microscopy. Cells were carefully rinsed 3 times with cold PBS and fixed for 20 min with PBS 4% formaldehyde.

2.4. Viability assay

Cell viability was assayed with the CellTiter-Glo Luminescent Cell Viability Assay (Promega, Charbonnières-les-Bains, France) as described (Khoshal et al., 2019). Luminescence was measured with a spectrophotometer (TECAN Spark, Mannedorf, Switzerland).

2.5. Ribotoxicity analysis by in-cell-western

Ribotoxicity was measured using protein synthesis inhibition as a surrogate. The measurement of protein synthesis by puromycin labelling was performed as described (Henrich, 2016). Puromycin was immuno-detected by In-Cell-Western using an anti-puromycin antibody (clone 12D10 diluted 1:5000; Millipore, Molseihm, France). GAPDH, which is constitutively expressed and has a half-life of 8 h (Dani et al., 1984), was used as a control. The anti GAPDH antibody was diluted 1:5000 (ABS16; Millipore). Secondary antibodies were diluted 1:5000 (IRDye 800 C W; Rockland, and IRDye 680RD Licor). Puromycin signal was normalized with the average fluorescence of puromycin-labelled control cells (Henrich, 2016).

2.6. Quantification of DNA damage by in-cell-western

In-Cell-Western was performed as previously described (Tronnet and Oswald, 2018). Fixed cells were permeabilized and stained with the primary antibody anti-γH2AX (20E3 diluted 1:200; Cell Signalling, Saint-Quentin en Yvelines, France). Secondary antibody (IRDye 800 C W diluted 1:1000; Rockland) and RedDot2 DNA marker (Biotium) were measured at 680 and 800 nm with a Sapphire Biomolecular Imager (Azure Biosystems). The genotoxic index was calculated by dividing the γH2AX signal by the corresponding DNA fluorescence and normalized with the average signal in control cells (Tronnet and Oswald, 2018).

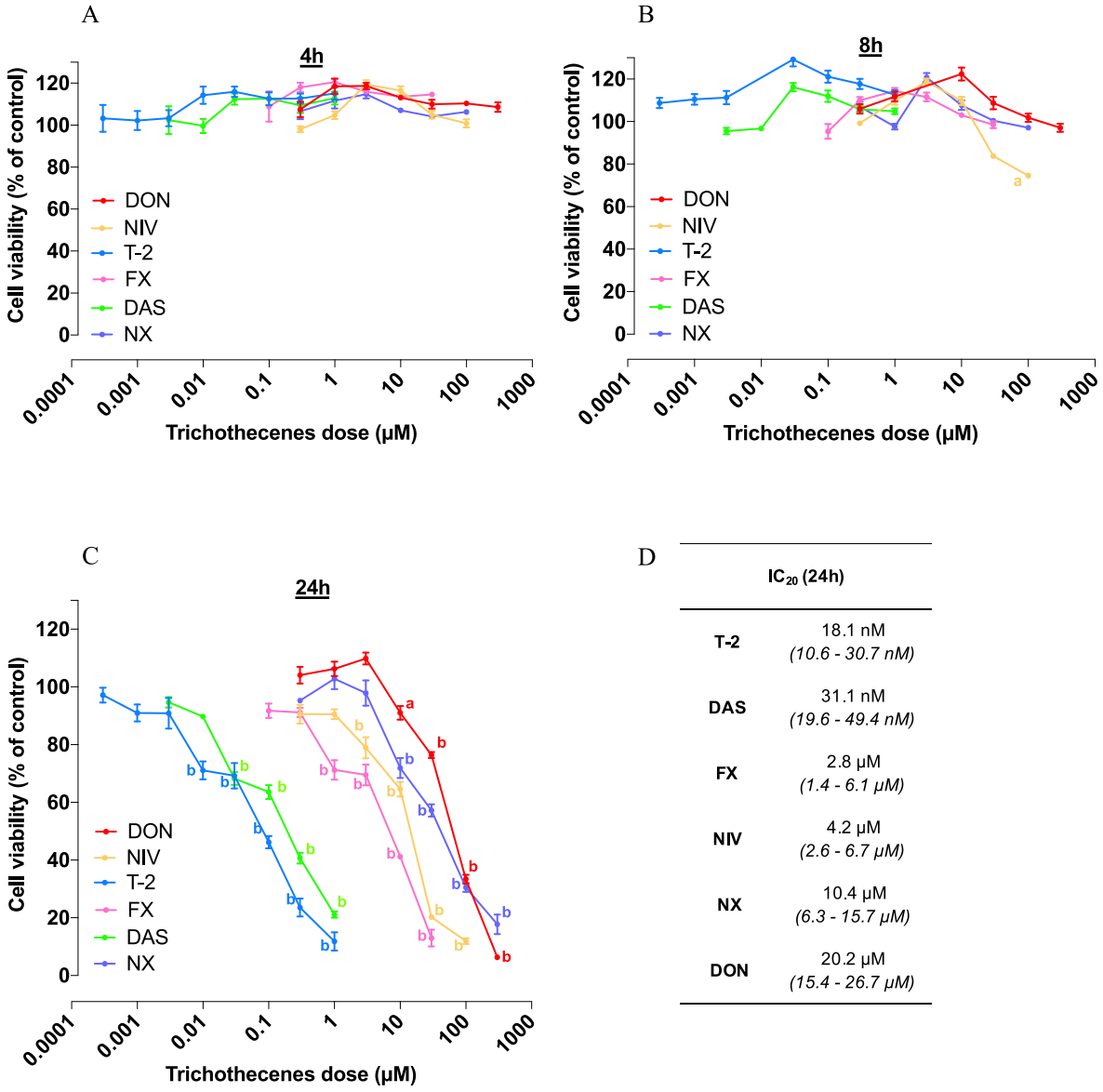

D

	IC_{20} (24h)
T-2	18.1 nM *(10.6 - 30.7 nM)*
DAS	31.1 nM *(19.6 - 49.4 nM)*
FX	2.8 µM *(1.4 - 6.1 µM)*
NIV	4.2 µM *(2.6 - 6.7 µM)*
NX	10.4 µM *(6.3 - 15.7 µM)*
DON	20.2 µM *(15.4 - 26.7 µM)*

Fig. 2. Trichothecenes are not cytotoxic after 4h and 8h treatment but induce dose-dependent cytotoxicity after 24h treatment of cultured intestinal cells. A, B, D: non-transformed rat intestinal epithelial IEC-6 cells were treated for 4 h (panel A), 8 h (panel B) and 24 h (panel C) with various concentrations of TCT and then viability was assessed by measuring cellular ATP levels. Data are expressed as mean ± SEM (3–6 independent experiments). P-values were calculated using one-way ANOVA with Bonferroni's multiple comparison (compared to the vehicle control cells), a: $p < 0.01$; b: $p < 0.0001$. D: concentrations that inhibited cell viability by 20% (IC_{20}) were calculated from the data presented in panel C. 95% confidence intervals are shown in italics.

2.7. Data analysis

GraphPad Prism 8.0 was used to calculate concentrations that inhibited the cell viability by 20% (IC_{20}), and the protein synthesis by 20% (20% PSI level), performing a four-parameter nonlinear regression model (sigmoidal dose-response analysis). Profile-likelihood confidence intervals were calculated from the nonlinear regressions. One-way analysis of variance (ANOVA) followed by Bonferroni's multiple comparison were performed. The data are expressed as mean ± SEM.

3. Results

3.1. Trichothecenes induce a dose-dependent reduction in cell viability

As the intestinal tract is the primary target of TCT, the non-transformed intestinal epithelial cell line IEC-6 was used. Cytotoxicity was first evaluated 4 h and 8 h after TCT treatment, and no cytotoxicity was detected (Fig. 2A and B). The effect of TCT on cell viability was then evaluated 24 h after treatment, and we observed a dose-dependent inhibition of viability induced by DON, NIV, T-2, FX, DAS, and NX (Fig. 2C). IC_{20} values, which correspond to the dose inducing a 20% reduction of cell viability, were calculated for each TCT (Fig. 2D). For cytotoxicity, TCT were classified as follows: T-2>DAS > FX > NIV > NX > DON.

3.2. Trichothecenes induce a dose-dependent ribotoxicity

Ribotoxicity is the main mode of action of TCT (Pestka, 2010). To quantify the ribotoxicity of the TCT, we examined translational inhibition, assessed by the incorporation of the protein translation marker puromycin in newly synthesized peptides (Henrich, 2016). The incorporated puromycin was quantified by immunofluorescence. All the TCT induced a dose-dependent ribotoxicity (Fig. 3A). Treatment with TCT did not induce a drop in GAPDH levels (which has an 8 h half-life), confirming that puromycin specifically labelled newly synthesized peptides (Fig. 3A, Fig. S3). The doses inducing a 20% reduction in protein synthesis were calculated (Fig. 3B). For their ribotoxic effect, the TCT were classified as follows: T-2>DAS > FX > NIV > NX ≥ DON.

3.3. Trichothecenes exacerbate the DNA damage induced by the drug phleomycin

The genotoxic exacerbation properties of TCT were first evaluated with phleomycin (PHM), a genotoxin commonly used as a model for genotoxicity assessments (Chen and Stubbe, 2005). IEC-6 cells were treated for 4 h with PHM and/or TCT. As expected, cells treated with PHM alone exhibited DNA damage signalled by the γH2AX marker (Rogakou et al., 1998). TCT alone did not induce γH2AX, indicating that they are not genotoxic by themselves. In contrast, all the trichothecenes induced exacerbation of PHM-induced DNA damage, in a dose-dependent manner (Fig. 4A). A significant increase occurred from 1 μM for DON, 3 μM for NX, 10 nM for T-2, 0.3 μM for FX, 30 nM for DAS,

A

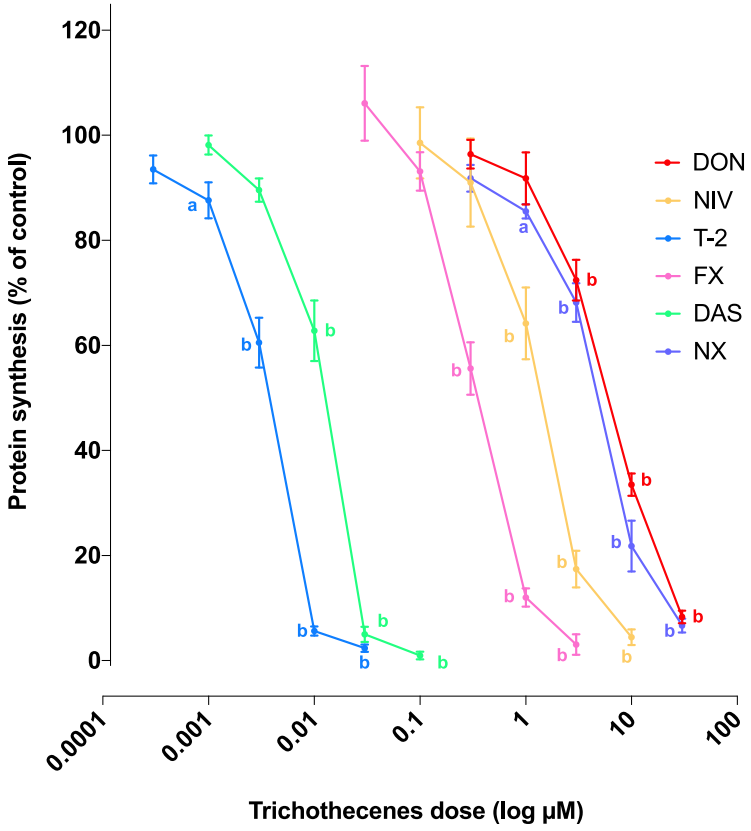

B

20% PSI level	
T-2	1.9 nM *(1.6 - 2.3 nM)*
DAS	6 nM *(5 - 7 nM)*
FX	0.15 μM *(0.12 - 0.19 μM)*
NIV	0.6 μM *(0.4 - 0.9 μM)*
NX	2.5 μM *(2.0 - 3.1 μM)*
DON	2.9 μM *(2.2 - 3.9 μM)*

Fig. 3. Trichothecenes induce dose-dependent ribotoxicity in cultured intestinal epithelial cells. A: IEC-6 cells were treated for 4 h with different concentrations of TCT and then the cells were treated for 30 min with puromycin, a protein translation marker. Incorporation of puromycin into newly synthesized peptides was quantified with an anti-puromycin antibody by In-Cell-Western. All the data are expressed as mean ± SEM (4 independent experiments). Values that are significantly different compared to the vehicle control are indicated a: $p < 0.01$; b: $p < 0.0001$: B: Concentrations that inhibited the protein synthesis by 20% (20% PSI) were calculated from the data shown in panel A. 95% confidence intervals are shown in italics.

A

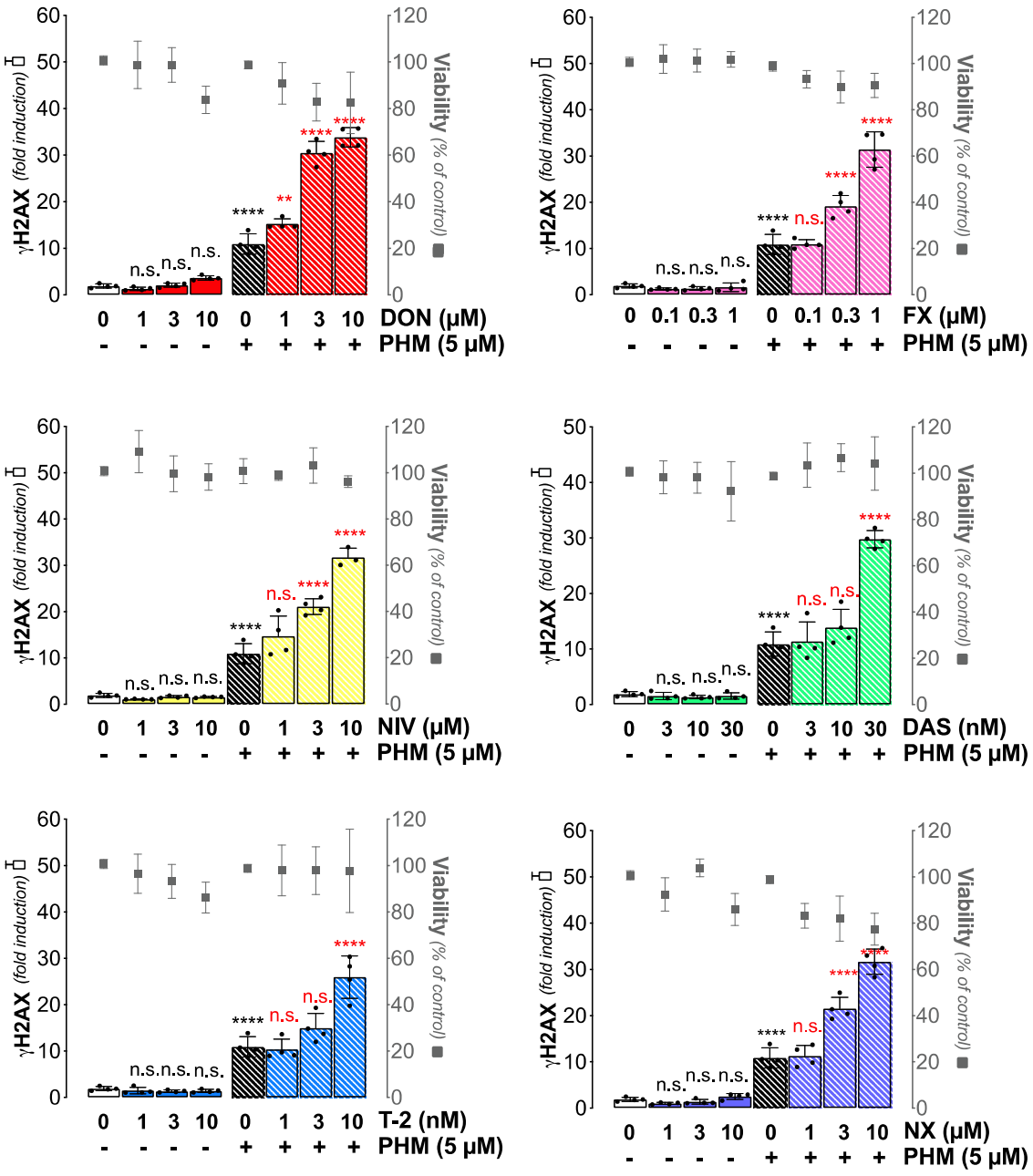

B

No effect dose					
T-2	DAS	FX	NIV	DON	NX
3 nM	10 nM	0.1 μM	1 μM	< 1 μM	1 μM

(caption on next page)

Fig. 4. Trichothecenes exacerbate the genotoxicity induced by the DNA-damaging drug phleomycin in a dose-dependent manner. A: IEC-6 cells were co-treated for 4 h with 5 μM phleomycin (PHM) and increasing doses of DON (red), NIV (yellow), T-2 (blue), FX (pink), DAS (green), or NX (purple). Then, DNA damage was measured by quantification of H2AX phosphorylation by In-Cell-Western. γH2AX fold induction (bars) is presented on the left Y axis, and the corresponding cells viability, measured through DNA quantification (grey squares) is presented on the right Y axis. All data are expressed as mean ± SEM (4 independent experiments). For γH2AX data, P-values were calculated using a one-way ANOVA with Bonferroni's multiple comparison. Values that are significantly different compared to vehicle are indicated by black asterisks, and values that are significantly different from infected cells without TCT are indicated by red asterisks. *:$p < 0.1$; **: $p < 0.01$; ***: $p < 0.001$, ****: $p < 0.0001$, n. s.: not significant. B: No exacerbation doses for each TCT was defined from data in panel A. (For interpretation of the references to colour in this figure legend, the reader is referred to the Web version of this article.)

and 3 μM for NX (Fig. 4B). The DNA damage exacerbation was confirmed in cells co-treated with phleomycin and a TCT-A (T-2 toxin) or a TCT-B (NIV), by detection of increased formation of 53BP1 foci and phosphorylation of RPA32, both markers of DNA damage (Vignard et al., 2013) (Dueva and Iliakis, 2020) (Supplementary methods 1, Fig. S1). The exacerbation of genotoxicity did not induce cell detachment, indicating that this effect was not a consequence of massive cell death (Fig. 4).

3.4. Trichothecenes exacerbate DNA damage induced by captan, a pesticide which contaminates food

We then tested the ability of TCT to exacerbate genotoxicity induced by a food-contaminating genotoxin, the pesticide captan, which can be found in fruits, vegetables, and cereals (Shinde et al., 2019). For this purpose, IEC-6 cells were exposed to captan and/or TCT for 4 h. Captan induced DNA damage on its own, and TCT induced an exacerbation of the genotoxicity of captan, in a dose-dependent manner. A significant increase occurred from 3 μM for DON and NX, 1 nM for T-2, 1 μM for FX, and 3 nM for DAS, and did not induce cell death (Fig. 5). The captan-induced genotoxicity exacerbation phenotype was confirmed by the increase of the 53BP1 and pRPA32 foci formation (Fig. S1).

3.5. Trichothecenes exacerbate the genotoxicity induced by colibactin, a genotoxin produced by members of the intestinal microbiota

We then determined whether TCT also exacerbate the genotoxicity induced by a bacterial genotoxin produced by the intestinal microbiota, colibactin. The genotoxicity of colibactin was measured by infecting IEC-6 cells with the live colibactin-producing bacterium *Escherichia coli* NC101. A direct contact between live colibactin-producing *E. coli* strain and eukaryotic cells is required to observe DNA damage (Chagneau et al., 2022; Nougayrède et al., 2006; Bossuet-Greif et al., 2018). Thus, cells were infected with strain NC101 and co-treated with TCT or not. Cells infected with *Escherichia coli* NC101showed an increase in their γH2AX signal, resulting from colibactin damage, whereas cells infected with the NC101 Δ*clbP* isogenic mutant, which is impaired for colibactin synthesis, did not exhibit DNA damage (Fig. 6, Fig. S2). In contrast, TCT-treated and NC101-infected cells exhibited an exacerbation of colibactin-induced DNA damage, which increased with the dose of TCT. A significant increase occurred at 3 μM for DON, NX and NIV, 1 nM for T-2, 0.3 μM for FX, and 10 nM for DAS (Fig. 6), and was not associated with cell death (Fig. 6). The exacerbation of colibactin-induced DNA damage by TCT-A and TCT-B was confirmed with the increased formation of 53BP1 and pRPA32 foci (Fig. S1). Exacerbation of DNA damage was not associated with increased colibactin production in bacteria treated with TCT, nor with an impact of TCT on bacterial growth (Supplementary methods 2, Fig. S2).

4. Discussion

Food contamination by TCT is a public health issue of the utmost importance. TCT levels in foods are indeed high and may even increase in the future, in part due to climate change (Van Der Fels-Klerx et al., 2016). DON, which is not genotoxic, was recently described as a genotoxicity enhancer (Garofalo et al., 2022; Payros et al., 2017). In this work, we show that this is not only an effect caused by DON, but also a novel effect attributable to at least five other TCT: NIV, T-2, FX, DAS and the recently discovered NX toxin. We examined the enhancement of genotoxicity by TCT in proliferating intestinal IEC-6 cells, as transmission of gene mutations occurs in dividing cells (Tomasetti & Vogelstein, 2015). In addition, proliferating cells are more sensitive to DON than differentiated cells (Luo et al., 2021). We found that TCT exacerbated not only the genotoxicity induced by the model genotoxin phleomycin, but also the genotoxicity induced by genotoxins from multiple exposure sources. Indeed, captan is a dietary fungicide with genotoxic properties, and colibactin is a bacterial genotoxin produced in the gut. For this newly identified effect, TCT were classified as follows: T-2>DAS > FX > NIV ≥ DON ≥ NX.

The cytotoxicity of TCT was compared in non-transformed IEC-6 intestinal cells. Our data show that trichothecenes, which were not cytotoxic after a treatment lasting 4 h or 8 h, induced a dose-dependent inhibition of cell viability after 24 h. These data allowed the classification of trichothecenes as follows: T-2>DAS > FX > NIV > NX > DON. Although to the best of our knowledge this is the first direct comparison and ranking of TCT cytotoxicity in IEC-6 cells, the classification is consistent with the literature. T-2 toxin is indeed known as the most toxic TCT, with IC_{20} about 1000 times greater than others (Fernández-Blanco et al., 2018). DAS is slightly less cytotoxic than T-2, but more than FX (Moon et al., 2003), and FX is more cytotoxic than NIV and DON (Aupanun et al., 2019; Alassane-Kpembi et al., 2017a). We observed that IEC-6 cells exhibit a modest sensitivity to DON. Indeed, after 24 h of treatment, we found an IC_{20} of 20.2 μM when others found IC_{20} of ≈0.5 μM in IPEC-1 cells, or ≈3 μM in Caco-2 cells (Alassane-Kpembi et al., 2015; Pierron et al., 2022). Our results are consistent with those obtained by Bianco et al., who found an IC_{50} for DON of 50.2 μM in IEC-6 cells, confirming the limited sensitivity of this cell line (Bianco et al., 2012). In addition, our results highlight that NX is approximately twice as cytotoxic as DON in IEC-6 cells. This result is consistent with the results of Pierron et al. which showed a higher inflammatory potential for NX compared to DON in porcine intestinal explants (Pierron et al., 2022). In contrast, the literature shows that NX-induced cytotoxicity is comparable to that of DON in HT-29 and Caco-2 cells (Varga et al., 2018; Pierron et al., 2022). Importantly, the doses of TCT that were cytotoxic after 24 h of exposure were higher than the doses that exacerbate genotoxicity (Table 1). This indicates that non-cytotoxic doses of TCT exacerbate genotoxicity. Because DNA damage is a source of genetic mutations through repair errors, this result raises questions about the fate of these cells (Basu, 2018). Cells co-exposed to genotoxins and TCT survive and could therefore pursue their cell cycle and division following repair of DNA damage. Further studies are needed to examine whether cells co-exposed to TCT and genotoxins could accumulate mutations, ultimately resulting in cellular transformation.

In this work, we also classified trichothecenes for their ribotoxicity. The ranking T-2>DAS > FX > NIV > NX ≥ DON is coherent with the TCT structures. The most ribotoxic trichothecenes carry substitutions thought to improve binding to the ribosome, such as the isovaleryl group at C_8 in T-2 or the acetyl groups at C_4 and C_{15} in DAS (Wu et al., 2013; Wang et al., 2021). Differences in TCT ribotoxicity may also be related to divergences in structural rearrangements induced by ribosome binding (Garreau de Loubresse et al., 2014). Depending on the TCT structure, structural rearrangements could differ and induce variations in the mode of protein synthesis inhibition. We have previously suggested that DON-induced ribotoxicity is involved in the genotoxicity exacerbation

A

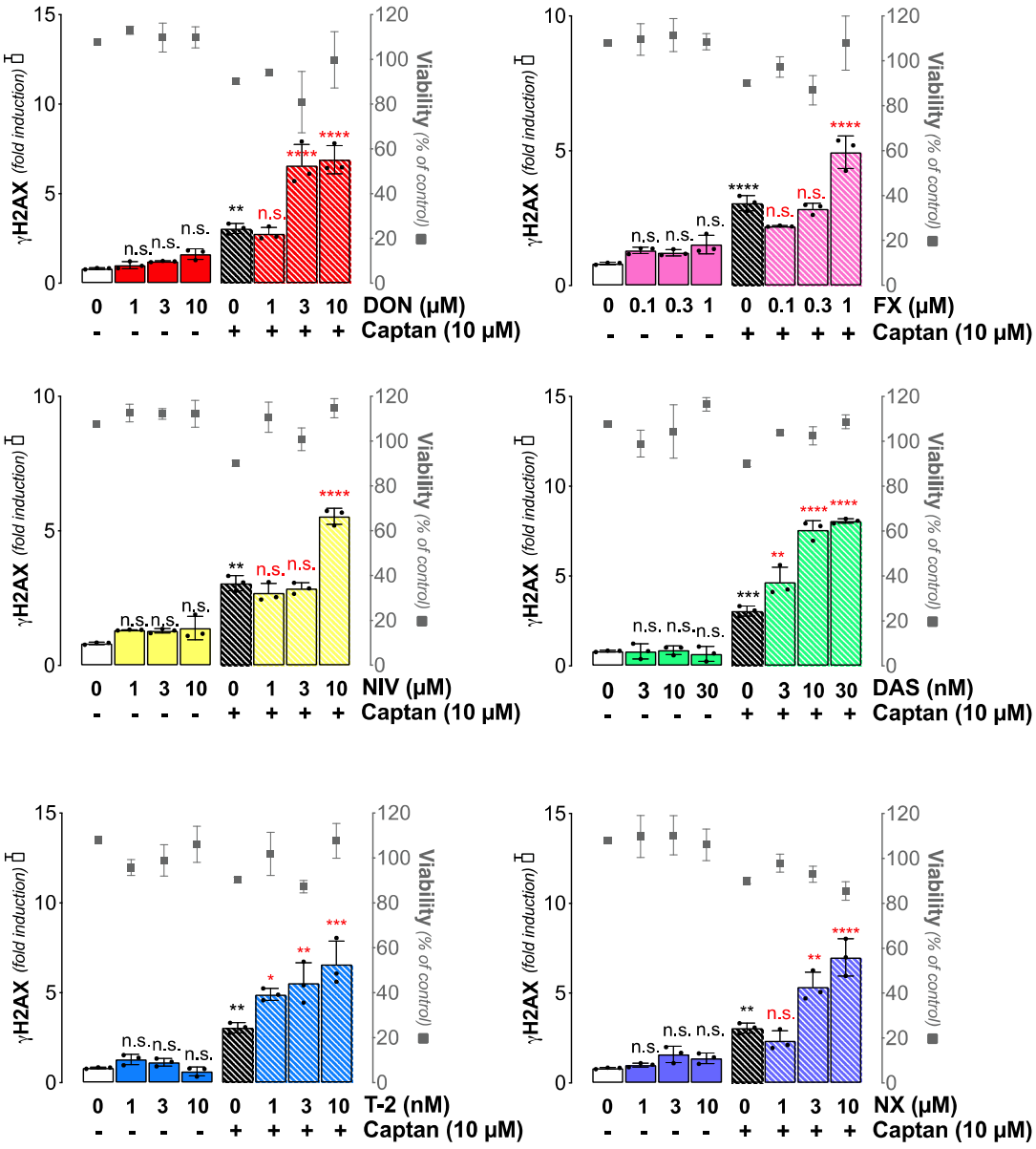

B

No effect dose					
T-2	DAS	FX	NIV	DON	NX
< 1 nM	< 3 nM	0.3 μM	3 μM	1 μM	1 μM

Fig. 5. Trichothecenes exacerbate the genotoxicity induced by the fungicide captan in a dose-dependent manner. A: IEC-6 cells were co-treated for 4 h with 10 μM captan and increasing doses of DON (red), NIV (yellow), T-2 (blue), FX (pink), DAS (green), or NX (purple). Then, DNA damage was measured by quantification of H2AX phosphorylation by In-Cell-Western. γH2AX fold induction (bars) is presented on the left Y axis, and the corresponding cell viability, measured through DNA quantification (grey squares) is presented on the right Y axis. All data are expressed as mean ± SEM (3 independent experiments). For γH2AX data, P-values were calculated using one-way ANOVA with Bonferroni's multiple comparison. Values that are significantly different compared to vehicle are indicated by black asterisks, and values that are significantly different from infected cells without TCT are indicated by red asterisks. *:$p < 0.1$; **: $p < 0.01$; ***: $p < 0.001$, ****: $p < 0.0001$, n. s.: not significant. B: No exacerbation dose for each TCT was determined from data shown in panel A. (For interpretation of the references to colour in this figure legend, the reader is referred to the Web version of this article.)

A

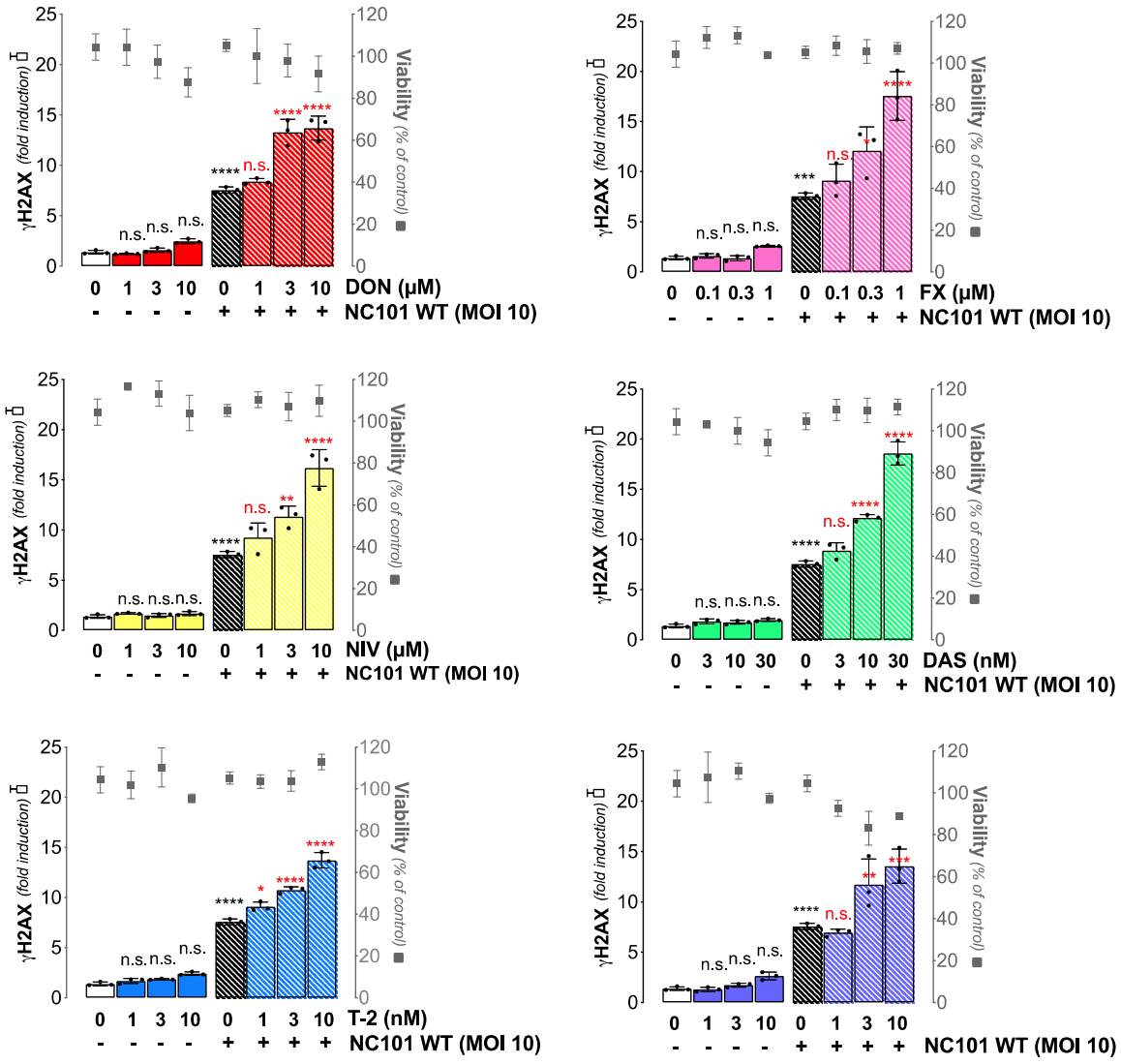

B

No effect dose					
T-2	DAS	FX	NIV	DON	NX
< 1 nM	3 nM	0.1 μM	0.3 μM	1 μM	1 μM

Fig. 6. Trichothecenes exacerbate the genotoxicity induced by the bacterial genotoxin colibactin in a dose-dependent manner. A: IEC-6 cells were infected 4 h with live colibactin-producing *E. coli* strain NC101 (multiplicity of infection of 10 bacteria per cell) with increasing doses of DON (red), NIV (yellow), T-2 (blue), FX (pink), DAS (green), or NX (purple). Cells were washed to remove bacteria and further incubated with the TCT for 4 h. Then, DNA damage was measured by quantification of H2AX phosphorylation by In-Cell-Western. γH2AX fold induction (bars) is presented on the left Y axis, and the corresponding cells viability, measured through DNA quantification (squares) is presented on the right Y axis. All data are expressed as mean ± SEM (3 independent experiments). For γH2AX data, P-values were calculated using one-way ANOVA with Bonferroni's multiple comparison. Values that are significantly different compared to vehicle are indicated by black asterisks, and values that are significantly different from infected cells without TCT are indicated by red asterisks. *: $p < 0.1$; **: $p < 0.01$; ***: $p < 0.001$, ****: $p < 0.0001$, n. s.: not significant. B: No exacerbation doses for each TCT was determined from data shown in Fig. 6A. (For interpretation of the references to colour in this figure legend, the reader is referred to the Web version of this article.)

Table 1
Trichothecenes classification for cytotoxicity, ribotoxicity, and capacity to exacerbate the genotoxicity. Green boxes: doses inducing no significant cytotoxicity at 4–24 h, ribotoxicy or genotoxicity exacerbation. Red boxes: doses inducing significant cytotoxicity, ribotoxicity or genotoxicity exacerbation.

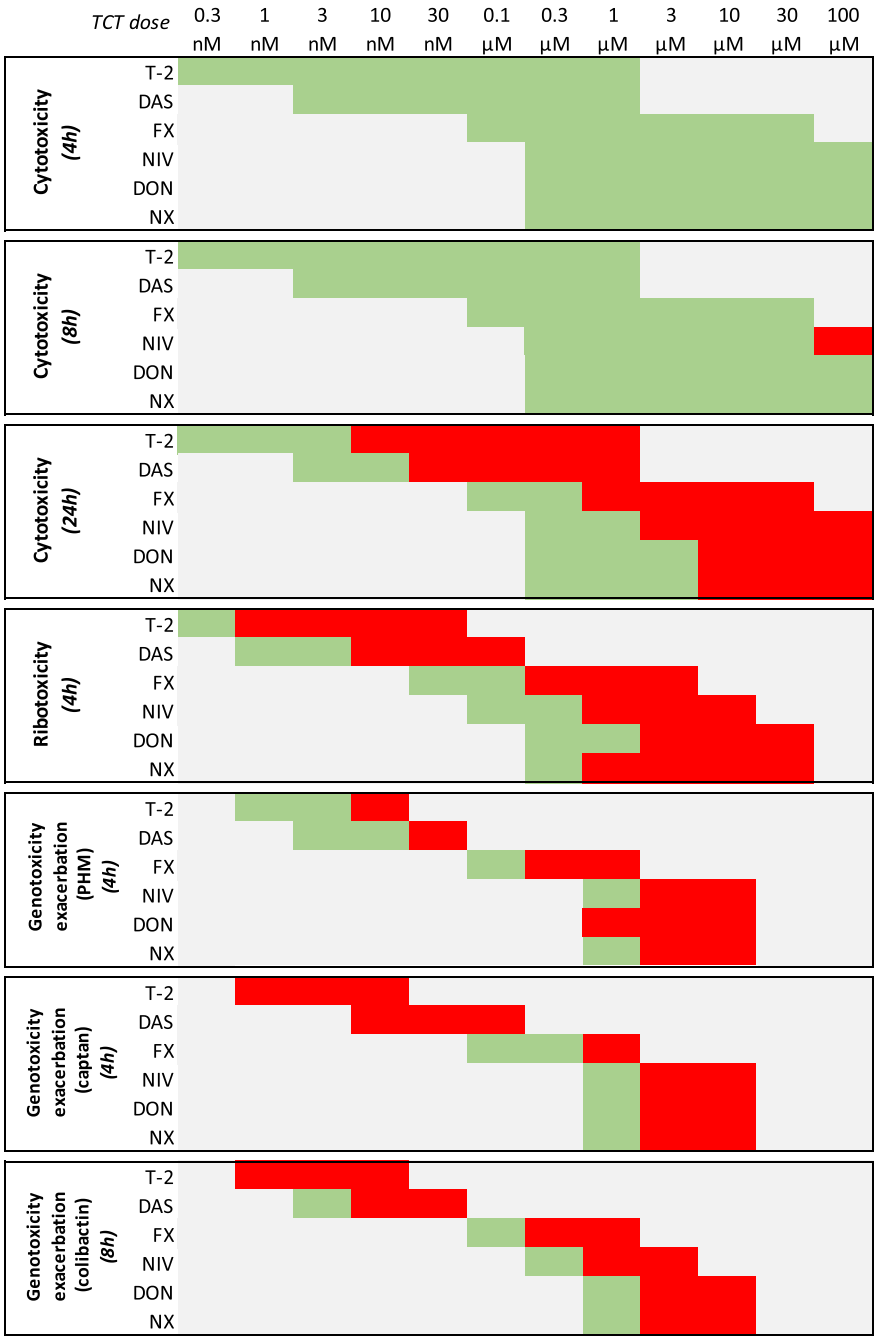

phenotype. Indeed, ribotoxic compounds reproduced the effect, while the non-ribotoxic DON derivative DOM-1, did not (Garofalo et al., 2022). The correlation between TCT ribotoxicity and genotoxicity exacerbating doses observed in this work (Table 1) support this hypothesis. Interestingly, TCT with substitutions that increase affinity to the ribosome have a greater capacity to exacerbate genotoxicity. This suggests that there is a structure-function link between ribotoxicity and genotoxicity exacerbation. TCT could be classified into 3 subgroups according to their capacity to exacerbate the genotoxicity, with regard to their affinity with the ribosome: T-2, DAS > FX > NIV, NX, DON. We also observed a parallel between ribotoxic and cytotoxic doses (Table 1). Ribosome inhibition is the main mechanism of action of TCT and is therefore probably the cause of cytotoxicity. This could be explained by the recruitment of MAP kinases in response to ribotoxic stress. Activated MAP kinases in turn activate apoptotic pathways (Yang et al., 2000).

Several mechanisms could be involved in the ribosome-dependent exacerbation of genotoxicity. In response to DNA damage, cells reprogram their gene expression to synthetize proteins of the DNA damage

response (Spriggs et al., 2010). TCT-induced ribotoxicity could disrupt the production of these stress response proteins. Through their ribotoxic effect, TCT can induce inflammation (Pestka, 2010; Garcia et al., 2018), which represses the DNA damage response (Jaiswal et al., 2000). Finally, it has been documented that DON activates the protein kinase R (PKR), which triggers the inhibition of the DNA damage repair and sensitizes cells to DNA damage (Zhou et al., 2014). As they share structural similarities with DON, TCT could also recruit PKR and induce sensitization to DNA damage. Further work is required to understand how ribotoxicity results in this novel TCT effect.

We observed that the exacerbation of genotoxicity occurred at realistic doses of TCT. The European Food Safety Authority (EFSA) established a no observable adverse effect level (NOAEL) for DON of 100 μg/kg body weight (bw)/day. This NOAEL was based on decreased feed intake and body weight in mice exposed to DON for two years (Knutsen et al. 2017a). For DAS, the NOAEL of 65 μg/kg bw/day is based on heamatotoxicity and immunotoxicity observed in cancer patients (Knutsen et al., 2018). The Benchmark Dose Limit ($BMDL_{05}$) for NIV, based on a reduction in white blood cells counts in a 90-day rat study, is 350 μg/kg bw/day (Knutsen et al., 2017b). The $BMDL_{10}$ for T-2, derived from reduction in the number of peripheral leucocytes in a sub chronic study in rats, is 3.3 μg/kg bw/day (Knutsen et al., 2017c). Estimating, like Maresca, 2013, that for a human weighing 70 kg, the small intestine content is 1 L, these doses can be converted to intestinal concentrations of 23.6 μM DON, 0.5 μM T-2, 12.4 μM DAS, and 78.4 μM NIV ((NOAEL or BMDL x 70)/molar mass of the TCT). Our study shows no effect doses for genotoxicity exacerbation well below these reference values, with 1 μM, 3 nM, 10 nM, and 3 μM for DON, T-2, DAS and NIV, respectively. In conclusion, genotoxicity exacerbation could occur at realistic doses of TCT. If confirmed, genotoxicity exacerbation should be considered as a sensitive endpoint for the definition of references values by EFSA. In addition, we observed that structurally related trichothecenes displayed comparable effects and could therefore be classified into 3 subgroups: T-2, DAS > FX > NIV, NX, DON. As TCT frequently co-occur in foodstuffs (Alassane-Kpembi et al., 2017b), it would be appropriate to set group TDIs for TCT, as it has been done for other groups of structurally related mycotoxins (Steinkellner et al. 2019).

We observed the genotoxicity exacerbation by TCT with three genotoxins from various sources and with different modes of action on DNA. Indeed, phleomycin is a radiomimetic drug which causes the oxidation of bases and strand breaks (Chen and Stubbe, 2005). Captan induces oxidative DNA damage and strand breaks (Fernandez-Vidal et al., 2019). Colibactin induces DNA interstrand crosslinks (Bossuet-Greif et al., 2018). Thus, this study confirms that the DNA damage exacerbation phenotype occurs with genotoxins with diverse modes of action (Garofalo et al., 2022).

The exacerbation effect occurred with captan, a pesticide which can contaminate fruits and vegetables, but also cereals, which are the main source of TCT (Shinde et al., 2019). Captan has been associated with multiple myeloma in farmers (Presutti et al., 2016), and is classified by the European Commission as "suspected of causing cancer" (European Commission, 2008). Notably, the exacerbation effect occurred at realistic doses of captan. The NOAEL for captan is indeed 25 mg/kg bw per day (based on reduced body weight gain in a two-year study in rats) (Anastassiadou et al., 2020), which corresponds to an intestinal concentration of 5.8 mM. Here, the exacerbated genotoxic effect of captan was observed with a dose as low as 10 μM, well below the NOAEL. Interestingly, TCT also exacerbate the effect of colibactin, an endogenous genotoxin produced by the intestinal microbiota throughout the host's life. Indeed, approximately 15% of 3-day-old neonates are colonized by colibactin-producing *E. coli* (Payros et al., 2014), and 25% of adults harbour these bacteria (Putze et al., 2009; Tenaillon et al., 2010; Johnson et al., 2008). In addition, the prevalence of the B2 phylogenetic group of *E. coli*, which includes up to 50% of colibactin-producing strains, is increasing in developed countries (Tenaillon et al., 2010). The intestinal microbiome also encodes other bacterial genotoxins such as cytolethal distending toxins (Taieb et al., 2016). Thus, humans are potentially co-exposed to TCT together with endogenous genotoxins produced by the microbiota as well as multiple exogenous diet-borne genotoxins, such as captan, alcohol-derivatives (Brooks and Zakhari, 2014), components of red meat (Bastide et al., 2011) and other genotoxic pesticides such as glyphosate (International Agency for Research on Cancer, 2017). Given the high prevalence of TCT in foods, it is conceivable that TCT could exacerbate the effect of the multiple genotoxic agents to which we are exposed.

5. Conclusion

We report that even though trichothecenes are not genotoxic by themselves, these contaminants promote the genotoxicity of genotoxins which are in the diet, such as pesticides, or are produced by the intestinal microbiota. Considering the wide prevalence of both TCT and genotoxins, a large portion of the population could be impacted by this novel effect. This is alarming because DNA damage drives cancer development (Basu, 2018). A preliminary report on a large-scale epidemiological study in the European Union has suggested a link between long-term exposure to DON and an increased risk of colon cancer (Huybrechts et al., 2019). If confirmed, the exacerbation of DNA damage by DON could be a key to explaining this epidemiological link. Here, we show that DON is not the only dietary TCT to exhibit this genotoxicity-exacerbating property. There is an urgent need for additional studies on the impact of TCT on carcinogenesis induced by other environmental toxicants.

Credit author statement

Marion Garofalo: Conceptualization, Methodology, Validation Formal analysis, Investigation, Writing - Original Draft, Visualization. **Delphine Payros**: Conceptualization, Methodology, Validation, Formal analysis, Investigation, Visualization. **Marie Penary:** Investigation, Validation. **Eric Ostwald**: Conceptualization, Writing - Review & Editing, Supervision, Fund Acquisition. **Jean-Philippe Nougayrede**: Conceptualization, Writing - Review & Editing, Supervision, Project administration, Fund Acquisition. **Isabelle P. Ostwald**: Conceptualization, Writing - Review & Editing, Supervision, Project administration, Fund Acquisition.

Declaration of competing interest

The authors declare that they have no known competing financial interests or personal relationships that could have appeared to influence the work reported in this paper.

Data availability

Data will be made available on request.

Acknowledgments

We thank David J. Miller for the gift of NX. We thank Julien Vignard (Toxalim) for the scientific input and help for immunofluorescence experiments. We are grateful to Elisha Oliver for editing the language. This work was supported by grants from the French Agence Nationale de la Recherche (Genofood ANR-19-CE34 and GenoMyc ANR-22-CE34). MG was supported by a fellowship from the French ministry for Higher Education and Research.

Appendix A. Supplementary data

Supplementary data to this article can be found online at https://doi.org/10.1016/j.envpol.2022.120625.

References

Aitken, A., Miller, J.D., McMullin, D.R., 2019. Isolation, chemical characterization, and hydrolysis of the trichothecene 7α-hydroxy, 15-deacetylcalonectrin (3ANX) from *Fusarium graminearum* DAOMC 242077. Tetrahedron Lett. 60, 852–856. https://doi.org/10.1016/j.tetlet.2019.02.025.

Alassane-Kpembi, I., Kolf-Clauw, M., Gauthier, T., Abrami, R., Abiola, F.A., Oswald, I.P., Puel, O., 2013. New insights into mycotoxin mixtures: the toxicity of low doses of Type B trichothecenes on intestinal epithelial cells is synergistic. Toxicol. Appl. Pharmacol. 272, 191–198. https://doi.org/10.1016/j.taap.2013.05.023.

Alassane-Kpembi, I., Puel, O., Oswald, I.P., 2015. Toxicological interactions between the mycotoxins deoxynivalenol, nivalenol and their acetylated derivatives in intestinal epithelial cells. Arch. Toxicol. 8, 1337–1346. https://doi.org/10.1007/s00204-014-1309-4.

Alassane-Kpembi, I., Gerez, J.R., Cossalter, A.M., Neves, M., Laffitte, J., Naylies, C., Lippi, Y., Kolf-Clauw, M., Bracarense, A.P.F.L., Pinton, P., Oswald, I.P., 2017a. Intestinal toxicity of the type B trichothecene mycotoxin fusarenon-X: whole transcriptome profiling reveals new signaling pathways. Sci. Rep. 7, 7530. https://doi.org/10.1038/s41598-017-07155-2.

Alassane-Kpembi, I., Puel, O., Pinton, P., Cossalter, A.M., Chou, T.C., Oswald, I.P., 2017b. Co-exposure to low doses of the food contaminants Deoxynivalenol and Nivalenol has a synergistic inflammatory effect on intestinal explants. Arch. Toxicol. 91, 2677–2687. https://doi.org/10.1007/s00204-016-1902-9.

Anastassiadou, M., Arena, M., Auteri, D., Brancato, A., Bura, L., Carrasco Cabrera, L., Chaideftou, E., Chiusolo, A., Crivellente, F., De Lentdecker, C., et al., 2020. Peer review of the pesticide risk assessment of the active substance captan. EFSA J. 18, 6230. https://doi.org/10.2903/j.efsa.2020.6230.

Aupanun, S., Poapolathep, S., Phuektes, P., Giorgi, M., Zhang, Z., Oswald, I.P., Poapolathep, A., 2019. Individual and combined mycotoxins deoxynivalenol, nivalenol, and fusarenon-X induced apoptosis in lymphoid tissues of mice after oral exposure. Toxicon 165, 83–94. https://doi.org/10.1016/j.toxicon.2019.04.017.

Bastide, N.M., Pierre, F.H., Corpet, D.E., 2011. Heme iron from meat and risk of colorectal cancer: a meta-analysis and a review of the mechanisms involved. Cancer Prev. Res. 4, 177–184. https://doi.org/10.1158/1940-6207.CAPR-10-0113.

Basu, A.K., 2018. DNA damage, mutagenesis and cancer. Int. J. Mol. Sci. 19, 970. https://doi.org/10.3390/ijms19040970.

Bianco, G., Fontanella, B., Severino, L., Quaroni, A., Autore, G., Marzocco, S., 2012. Nivalenol and deoxynivalenol affect rat intestinal epithelial cells: a concentration related study. PLoS One 7, e52051. https://doi.org/10.1371/journal.pone.0052051.

Bossuet-Greif, N., Vignard, J., Taieb, F., Mirey, G., Dubois, D., Petit, C., Oswald, E., Nougayrède, J.P., 2018. The colibactin genotoxin generates DNA interstrand cross-links in infected cells. mBio 9, e02393. https://doi.org/10.1128/mBio.02393-17.

Brooks, P.J., Zakhari, S., 2014. Acetaldehyde and the genome: beyond nuclear DNA adducts and carcinogenesis. Environ. Mol. Mutagen. 55, 77–91. https://doi.org/10.1002/em.21824.

Chagneau, C.V., Payros, D., Tang-Fichaux, M., Auvray, F., Nougayrède, J.P., Oswald, E., 2022. The pks island: a bacterial Swiss army knife? Trends Microbiol. https://doi.org/10.1016/j.tim.2022.05.01.

Chen, J., Stubbe, J., 2005. Bleomycins: towards better therapeutics. Nat. Rev. Cancer 5, 102–112. https://doi.org/10.1038/nrc1547.

Cundliffe, E., Davies, J.E., 1977. Inhibition of initiation, elongation, and termination of eukaryotic protein synthesis by trichothecene fungal toxins. Antimicrob. Agents Chemother. 11, 491–499. https://doi.org/10.1128/AAC.11.3.491.

Dani, C., Piechaczyk, M., Audigier, Y., El Sabouty, S., Cathala, G., Marty, L., Fort, P., Blanchard, J.M., Jeanteur, P., 1984. Characterization of the transcription products of glyceraldehyde 3-phosphate-dehydrogenase gene in HeLa cells. Eur. J. Biochem. 14, 299–304. https://doi.org/10.1111/j.1432-1033.1984.tb08552.x.

Dueva, R., Iliakis, G., 2020. Replication protein A: a multifunctional protein with roles in DNA replication, repair and beyond. NAR Cancer 2. https://doi.org/10.1093/narcan/zcaa022 zcaa022.

Eskola, M., Elliott, C.T., Hajšlov, J., Steiner, D., Krska, R., 2020. Towards a dietary-exposome assessment of chemicals in food: an update on the chronic health risks for the European consumer. Crit. Rev. Food Sci. Nutr. 60, 1890–1911. https://doi.org/10.1080/10408398.2019.1612320.

European Commission, 2008. Regulation No 1272/2008 of the European Parliament and of the Council of 16 December 2008 on classification, labelling and packaging of substances and mixtures, amending and repealing Directives 67/548/EEC and 1999/45/EC and amending Regulation (EC) No 1907/2006. Off. J. Eur. Union 354, 1–1355.

Fernández-Blanco, C., Elmo, L., Waldner, T., Ruiz, M.J., 2018. Cytotoxic effects induced by patulin, deoxynivalenol and toxin T2 individually and in combination in hepatic cells (HepG2). Food Chem. Toxicol. 120, 12–23. https://doi.org/10.1016/j.fct.2018.06.019.

Fernandez-Vidal, A., Arnaud, L.C., Maumus, M., Chevalier, M., Mirey, G., Salles, B., Vignard, J., Boutet-Robinet, E., 2019. Exposure to the fungicide captan induces DNA base alterations and replicative stress in mammalian cells. Environ. Mol. Mutagen. 3, 286–297. https://doi.org/10.1002/em.22268.

Foroud, N.A., Baines, D., Gagkaeva, T.Y., Thakor, N., Badea, A., Steiner, B., Bürstmayr, M., Bürstmayr, H., 2019. Trichothecenes in cereal grains – an update. Toxins 11, 634. https://doi.org/10.3390/toxins11110634.

Garcia, G.R., Payros, D., Pinton, P., Dogi, C.A., Laffitte, J., Neves, M., Gonzalez-Pereyra, M.L., Cavaglieri, L.R., Oswald, I.P., 2018. Intestinal toxicity of deoxynivalenol is limited by *Lactobacillus rhamnosus* RC007 in pig jejunum explants. Arch. Toxicol. 92, 983–993. https://doi.org/10.1007/s00204-017-2083-x.

Garreau de Loubresse, N., Prokhorova, I., Holtkamp, W., Rodnina, V., Yusupova, G., Yusupov, M., 2014. Structural basis for the inhibition of the eukaryotic ribosome. Nature 513, 517–522. https://doi.org/10.1038/nature13737.

Garofalo, M., Payros, D., Oswald, E., Nougayrède, J.P., Oswald, I.P., 2022. The foodborne contaminant deoxynivalenol exacerbates DNA damage caused by a broad spectrum of genotoxic agents. Sci. Total Environ. 820, 153280 https://doi.org/10.1016/j.scitotenv.2022.153280.

Gottschalk, C., Bauer, J., Meyer, K., 2008. Detection of satratoxin g and h in indoor air from a water-damaged building. Mycopath 166, 103–107. https://doi.org/10.1007/s11046-008-9126-z.

Henrich, C.J., 2016. A microplate-based nonradioactive protein synthesis assay: application to TRAIL sensitization by protein synthesis inhibitors. PLoS One 11, e0165192. https://doi.org/10.1371/journal.pone.0165192.

Huybrechts, K., Claeys, L., Ferrari, P., Altieri, A., Arcella, D., Papadimitriou, C., Casagrande, C., Nicolas, G., Biessy, C., Zavadil, J., Gunter, M., De Saeger, S., De Boevre, M., 2019. Impact of Chronic Multi-Mycotoxin Dietary Exposure on Colorectal and Liver Cancer Risk in Europe. World Mycotoxin Forum - Book of Abstracts, p. 70.

International Agency for Research on Cancer (IARC), 2017. Working Group on the Evaluation of Carcinogenic Risks to Humans. In: 'Some Organophosphate Insecticides and Herbicides', Lyon (FR), vol. 112. Bookshelf ID: NBK436774.

Jaiswal, M., Laurosso, N.F., Burgart, L.J., 2000. Inflammatory cytokines induce DNA damage and inhibit DNA repair in cholangiocarcinoma cells by a nitric oxide-dependent mechanism. Cancer Res. 60, 184–190.

Johnson, J.R., Johnston, B., Kuskowski, M.A., Nougayrede, J.P., Oswald, E., 2008. Molecular epidemiology and phylogenetic distribution of the Escherichia coli pks genomic island. J. Clin. Microbiol. 46, 3906–3911. https://doi.org/10.1128/JCM.00949-08.

Khoshal, A.K., Novak, B., Martin, P.G.P., Jenkins, T., Neves, M., Schatzmayr, G., Oswald, I.P., Pinton, P., 2019. Co-Occurrence of DON and emerging mycotoxins in worldwide finished pig feed and their combined toxicity in intestinal cells. Toxins 12, 727. https://doi.org/10.3390/toxins11120727.

Knutsen, H.K., Alexander, J., Barregard, L., Bignami, M., Bruschweiler, B., Ceccatelli, S., Cottrill, B., Dinovi, M., Grasl-Kraupp, B., Hogstrand, C., et al., 2017a. Risks to human and animal health related to the presence of deoxynivalenol and its acetylated and modified forms in food and feed. EFSA J. 15, e04718 https://doi.org/10.2903/j.efsa.2017.4718.

Knutsen, H.K., Barregard, L., Bignami, M., Bruschweiler, B., Ceccatelli, S., Cottrill, B., Dinovi, M., Edler, L., Grasl-Kraupp, B., Hogstrand, C., et al., 2017b. Appropriateness to set a group health based guidance value for nivalenol and its modified forms. EFSA J. 15, 4751. https://doi.org/10.2903/j.efsa.2017.4751.

Knutsen, H.K., Barregard, L., Bignami, M., Bruschweiler, B., Ceccatelli, S., Cottrill, B., Dinovi, M., Edler, L., Grasl-Kraupp, B., Hoogenboom, L., et al., 2017c. Appropriateness to set a group health based guidance value for T2 and HT2 toxin and its modified forms. EFSA J. 15, 4655. https://doi.org/10.2903/j.efsa.2017.4655.

Knutsen, H.K., Alexander, J., Barregard, L., Bignami, M., Bruschweiler, B., Ceccatelli, S., Cottril, B., Dinovi, M., Grasl-Kraupp, B., Hogstrand, C., et al., 2018. Risk to human and animal health related to the presence of 4,15-diacetoxyscirpenol in food and feed. EFSA J. 16, 8. https://doi.org/10.2903/j.efsa.2018.5367.

Luo, S., Terciolo, C., Neves, M., Puel, S., Naylies, C., Lippi, Y., Pinton, P., Oswald, I.P., 2021. Comparative sensitivity of proliferative and differentiated intestinal epithelial cells to the food contaminant, deoxynivalenol. Environ. Pollut. 277, 116818 https://doi.org/10.1016/j.envpol.2021.116818.

Luongo, D., Severino, L., Bergamo, P., D'Arienzo, R., Rossi, M., 2010. Trichothecenes NIV and DON modulate the maturation of murine dendritic cells. Toxicon 55, 73–80. https://doi.org/10.1016/j.toxicon.2009.06.039.

Maresca, M., 2013. From the gut to the brain: journey and pathophysiological effects of the food-associated trichothecene mycotoxin deoxynivalenol. Toxins 23, 784–820. https://doi.org/10.3390/toxins5040784.

Moon, Y., Uzarski, R., Pestka, J.J., 2003. Relationship of trichothecene structure to COX-2 induction in the macrophage: selective action of type B (8-keto) trichothecenes. J. Toxicol. Environ. Health A. 66, 1967–1983. https://doi.org/10.1080/713853950.

Nougayrède, J.P., Homburg, S., Taieb, F., Boury, M., Brzuszkiewicz, E., Gottschalk, G., Buchrieser, C., Hacker, J., Dobrindt, U., Oswald, E., 2006. *Escherichia coli* induces DNA double-strand breaks in eukaryotic cells. Science 313, 848–851. https://doi.org/10.1126/science.1127059.

Payros, D., Secher, T., Boury, M., Brehin, C., Ménard, S., Salvador-Cartier, C., Cuevas-Ramos, G., Watrin, C., Marcq, I., Nougayrède, J.P., et al., 2014. Maternally acquired genotoxic *Escherichia coli* alters offspring's intestinal homeostasis. Gut Microb. 5, 313–512. https://doi.org/10.4161/gmic.28932.

Payros, D., Alassane-Kpembi, I., Pierron, A., Loiseau, N., Pinton, P., Oswald, I.P., 2016. Toxicology of deoxynivalenol and its acetylated and modified forms. Arch. Toxicol. 90, 2931–2957. https://doi.org/10.1007/s00204-016-1826-4.

Payros, D., Dobrindt, U., Martin, P., Secher, T., Bracarense, A.P.F.L., Boury, M., Laffitte, J., Pinton, P., Oswald, E., Oswald, I.P., 2017. The food contaminant deoxynivalenol exacerbates the genotoxicity of gut microbiota. mBio 8, e007–e017. https://doi.org/10.1128/mBio.00007-17.

Payros, D., Garofalo, M., Pierron, A., Soler-Vasco, L., Al-Ayoubi, C., Maruo, V.M., Alassane- Kpembi, I., Pinton, P., Oswald, I.P., 2021a. Mycotoxins in human food: a challenge for research. Cah. Nutr. Diet. 56, 170–183. https://doi.org/10.1016/j.cnd.2021.02.001.

Payros, D., Alassane-Kpembi, I., Laffitte, J., Lencina, C., Neves, M., Bracarense, A.P., Pinton, P., Ménard, S., Oswald, I.P., 2021b. Dietary exposure to the food contaminant deoxynivalenol triggers colonic breakdown by activating the mitochondrial and the death receptor pathways. Mol. Nutr. Food Res. 65, e2100191 https://doi.org/10.1002/mnfr.202100191.

Pestka, J.J., 2010. Deoxynivalenol-induced proinflammatory gene expression: mechanisms and pathological sequelae. Toxins 2, 1300–1317. https://doi.org/10.3390/toxins2061300.

Pierron, A., Neves, M., Puel, S., Lippi, Y., Soler, L., Miller, J.D., Oswald, I.P., 2022. Intestinal toxicity of the new type A trichothecenes, NX and 3ANX. Chemosphere 288, 132415. https://doi.org/10.1016/j.chemosphere.2021.132415.

Pinton, P., Oswald, I.P., 2014. Effect of deoxynivalenol and other type B trichothecenes on the intestine: a review. Toxins 6, 1615–1643. https://doi.org/10.3390/toxins6051615.

Polak-Śliwińska, M., Paszczyk, B., 2021. Trichothecenes in food and feed, relevance to human and animal health and methods of detection: a systematic review. Molecules 26, 454. https://doi.org/10.3390/molecules26020454.

Presutti, R., Harris, S.A., Kachuri, L., Spinelli, J.J., Pahwa, M., Blair, A., Zahm, S.H., Cantor, K.P., Weisenburger, D.D., Pahwa, P., et al., 2016. Pesticide exposures and the risk of multiple myeloma in men: an analysis of the North American Pooled Project. Int. J. Cancer 139, 1703–1714. https://doi.org/10.1002/ijc.30218.

Putze, J., Hennequin, C., Nougayrède, J.P., Zhang, W., Homburg, S., Karch, H., Bringer, M.A., Fayolle, C., Carniel, E., Rabsch, W., Oelschlaeger, T.A., Oswald, E., Forestier, C., Hacker, J., Dobrindt, U., 2009. Genetic structure and distribution of the colibactin genomic island among members of the family *Enterobacteriaceae*. Infect. Immun. 77, 4696–4703. https://doi.org/10.1128/IAI.00522-09.

Rogakou, E.P., Pilch, D.R., Orr, A.H., Ivanova, V.S., Bonner, W.M., 1998. DNA double-stranded breaks induce histone H2AX phosphorylation on serine 139. J. Biol. Chem. 273, 5858–5868. https://doi.org/10.1074/jbc.273.10.5858.

Schothorst, R.C., van Egmond, H.P., 2003. Report from SCOOP task 3.2.10: collection of occurrence data of *Fusarium* toxins in food and assessment of dietary intake by the population of EU member states. Subtask: trichothecenes', *Toxicol. Lett.* 153, 133–143. https://doi.org/10.1016/j.toxlet.2004.04.045.

Seeboth, J., Solinhac, R., Oswald, I.P., Guzylack-Piriou, L., 2012. The fungal T-2 toxin alters the activation of primary macrophages induced by TLR-agonists resulting in a decrease of the inflammatory response in the pig. Vet. Res. 43, 35. https://doi.org/10.1186/1297-9716-43-35.

Shinde, R., Shiragave, P., Lakade, A., Thorat, P., Banerjee, K., 2019. Multi-residue analysis of captan, captafol, folpet, and iprodione in cereals using liquid chromatography with tandem mass spectrometry. Food Addit. Contam. Part A Chem. Anal. Control Expo. Risk Assess. 36, 1688–1695. https://doi.org/10.1080/19440049.2019.1662953.

Soler, L., Miller, I., Terciolo, C., Hummel, K., Nöbauer, K., Neves, M., Oswald, I.P., 2022. Exposure of intestinal explants to NX, but not to DON, enriches the secretome in mitochondrial proteins. Arch. Toxicol. https://doi.org/10.1007/s00204-022-03318-x.

Spriggs, K.A., Bushell, M., Willis, A.E., 2010. Translational regulation of gene expression during conditions of cell stress. Mol. Cell 40, 228–237. https://doi.org/10.1016/j.molcel.2010.09.028.

Steinkellner, H., Binaglia, M., Dall'Asta, C., Gutleb, A.C., Metzler, M., Oswald, I.P., Parent-Massin, D., Alexander, J., 2019. Combined hazard assessment of mycotoxins and their modified forms applying relative potency factors: zearalenone and T2/HT2 toxin. Food Chem. Toxicol. 131, 110599 https://doi.org/10.1016/j.fct.2019.110599.

Taieb, F., Petit, C., Nougayrède, J.P., Oswald, E., 2016. The enterobacterial genotoxins: cytolethal distending toxin and colibactin. EcoSal Plus 7, 1. https://doi.org/10.1128/ecosalplus.ESP-0008-2016. PMID: 27419387.

Tani, N., Dohi, Y., Onji, Y., Yonemasu, K., 1995. Antiviral activity of trichothecene mycotoxins (deoxynivalenol, fusarenon-X, and nivalenol) against herpes simplex virus types 1 and 2. Microbiol. Immunol. 39, 635–637. https://doi.org/10.1111/j.1348-0421.1995.tb02254.x.

Tenaillon, O., Skurnik, D., Picard, B., Denamur, E., 2010. The population genetics of commensal *Escherichia coli*. Nat. Rev. Microbiol. 8, 207–217. https://doi.org/10.1038/nrmicro2298.

Terciolo, C., Maresca, M., Pinton, P., Oswald, I.P., 2018. Review article: role of satiety hormones in anorexia induction by Trichothecene mycotoxins. Food Chem. Toxicol. 121, 701–714. https://doi.org/10.1016/j.fct.2018.09.034.

Tomasetti, C., Vogelstein, B., 2015. Variation in cancer risk among tissues can be explained by the number of stem cell divisions. Science 6217, 78–81. https://doi.org/10.1126/science.1260825.

Tronnet, S., Oswald, E., 2018. Quantification of colibactin-associated genotoxicity in HeLa cells by in cell western (ICW) using γ-H2AX as a marker. Bio Protoc 8, e2771. https://doi.org/10.21769/BioProtoc.2771.

Van Der Fels-Klerx, H.J., Liu, C., Battilani, P., 2016. Modelling climate change impacts on mycotoxin contamination. World Mycotoxin J. 5, 717–726. https://doi.org/10.3920/WMJ2016.2066.

Varga, E., Wiesenberger, G., Hametner, C., Ward, T.J., Dong, Y., Schöfbeck, D., McCormick, S., Broz, K., Stückler, R., Schuhmacher, R., et al., 2015. New tricks of an old enemy: isolates of *Fusarium graminearum* produce a type A trichothecene mycotoxin. Environ. Microbiol. 17, 2588–2600. https://doi.org/10.1111/1462-2920.12718.

Varga, E., Wiesenberger, G., Woelflingseder, L., Twaruschek, K., Hametner, C., Vaclaviková, M., Malachová, A., Marko, D., Berthiller, F., Adam, G., 2018. Less-toxic rearrangement products of NX-toxins are formed during storage and food processing. Toxicol. Lett. 284, 205–212. https://doi.org/10.1016/j.toxlet.2017.12.016.

Vignard, J., Mirey, G., Salles, B., 2013. Ionizing-radiation induced DNA double-strand breaks: a direct and indirect lighting up. Radiother. Oncol. 108, 362–369. https://doi.org/10.1016/j.radonc.2013.06.013.

Wang, W., Zhu, Y., Abraham, N., Li, X.Z., Kimber, M., Zhou, T., 2021. The ribosome-binding mode of trichothecene mycotoxins rationalizes their structure—activity relationships. Int. J. Mol. Sci. 22, 1604. https://doi.org/10.3390/ijms22041604.

Weaver, G.A., Kurtz, H.J., Bates, F.Y., Mirocha, C.J., Behrens, J.C., Hagler, W.M., 1981. Diacetoxyscirpenol toxicity in pigs. Res. Vet. Sci. 31, 131–135. https://doi.org/10.1016/S00345288(18)32480-9.

Wu, Q., Dohnal, V., Kuca, K., Yuan, Z., 2013. Trichothecenes: structure-toxic activity relationships. Curr. Drug Metabol. 14, 641–660. https://doi.org/10.2174/1389200211314060002.

Wyatt, R.D., Hamilton, P.B., Burmeister, H.R., 1973. The effects of T-2 toxin in broiler chickens. Poultry Sci. 52, 1853–1859. https://doi.org/10.3382/ps.0521853.

Yang, G.H., Jarvis, B.B., Chung, Y.J., Pestka, J.J., 2000. Apoptosis induction by the satratoxins and other trichothecene mycotoxins: relationship to ERK, p38 MAPK, and SAPK/JNK activation. Tox. appl. pharmacol. 164, 149–160. https://doi.org/10.1006/taap.1999.8888.

Yang, Y., Gharaibeh, R.Z., Newsome, R.C., Jobin, C., 2020. Amending microbiota by targeting intestinal inflammation with TNF blockade attenuates development of colorectal cancer. Nat. Can. (Que.) 7, 723–734. https://doi.org/10.1038/s43018-020-0078-7.

Zhou, H.R., He, K., Landgraf, J., Pan, X., Pestka, J.J., 2014. Direct activation of ribosome-associated double-stranded RNA-dependent protein kinase (PKR) by deoxynivalenol, anisomycin and ricin: a new model for ribotoxic stress response induction. Toxins 6, 3406–3425. https://doi.org/10.3390/toxins6123406.